National Academy of Sciences of Ukraine
Institute of Mathematics

Preprint 97.11

Yu.A. Mitropolsky,
A.A. Berezovsky, Yu.V. Zhernovyi

FREE BOUNDARY PROBLEMS AND MATHEMATICAL MODELLING OF ELECTRON-BEAM AUTOCRUCIBLE MELTING

Kyiv–97

FREE BOUNDARY PROBLEMS AND MATHEMATICAL MODELLING OF ELECTRON-BEAM AUTOCRUCIBLE MELTING/ Yu.A.Mitropolsky, .A.A.Berezovsky, Yu.V.Zhernovyi.- Kyiv, 1997. - 32 p.

Simplified one-dimensional and two-dimensional axisymmetric mathematical models which essentially correspond adequately to the thermophysical model of the electron-beam autocrucible melting are developed and examined. To solve the one-dimensional nonstationary Stefan problem a variational method essentially using a construction of the exact solution of the steady-state Stefan problem is applied. With the help of Kirchhoff transformation and the Green function the axisymmetric steady-state problem is reduced to a nonlinear integral Hammerstein equation. Here, a dependence of the thermal conductivity coefficient on the temperature on the surfaces being cooled is not taken into account but constant (mean) values of λ_s are utilized. To solve the problem in the case where this dependence $\lambda_s(T)$ is taken into account a auxiliary Green function method is proposed which also permits to take into account a change of the heat exchange coefficients on the autocrucible surfaces being cooled as well as to reduce the problem to a system of three integral Hammerstein equations. Numerical solutions of the nonlinear integral equations are obtained with the help of a variational (projective-net) method for the case of a circular scan of an electron beam over the heating surface. Results obtained by means of computations are well consistent with experimental data.

The bibliographi: 14 titles.

Reviewer: Igor T.Selezov

1. INTRODUCTION

To produce refractory metals and alloys one can use vacuum electron-beam autocrucible melting (EBAM) which is one of the special methods of casting. The main advantage of this method (in comparison with others methods of the special electrometallurgy) is a higher degree of metal refining from harmful admixtures, nonmetallic and gas inclusions. Complexity of thermal, hydrodynamical and physicochemical processes in an autocrucible, high temperatures, profound vacuum not only essentially complicate experimental studies of temperature fields in a melted portion of material but also, for some refractory metals, make such studies problematical. In this connection, besides experimental methods, mathematical methods of computation and prediction of thermal and kinetic characteristics of the melting process play a decisive role.

An autocrucible has a cylindrical form (Fig.1), its lateral surface ($r=a$) and bottom surface ($z=0$) are cooled, and energy absorption of the electron-beam heating with a flux density q occurs on the surface $z=l$ in the focal spot of radius $b<a$. The obtained thermal energy is spent on metal heating, on melting heat, that can be represented by heat flows distributed along a melting isotherm (a interface between the solid and liquid phases) with a constant linear density. Besides, heat exchange with enclosing medium (a contour being cooled by water) by means of conduction and radiation in a relation being difficultly controlled occurs from the lateral and bottom surfaces. The heat losses by means of radiation and evaporation take place from the surface being heated.

The EBAM is realized with application of the melt electromagnetic stirring (MEMS) over the whole volume of the liquid pool enabling to increase the end metal discharge. Complete mathematical models in the form of a set of differential equations of heat and mass transfer with account of hydrodynamic and electromagnetic processes can be used for melting process modeling. Such models are extremely laborious and their numerical realization needs much expenses of machine time. In order to determine basic technological parameters of the EBAM process on the basis of numerical calculati-

ons it is advantageous to use simplified mathematical models [1-8] based on special statements of heat conduction problems including phase change metal-melt (Stefan problems). It is necessary to find temperature fields in solid and liquid metal as well as its moving isothermal surface on which absorption of the melting heat takes place.

2. MATHEMATICAL MODELS WITH ONE SPACE VARIABLE

If the focal spot is a circle then the temperature field is axisymmetric, $T=T(r,z,t)$. The MEMS application approximate it to spherically symmetric. In this connection, for approximate calculations of a liquid pool dynamics we can restrict ourselves to consideration the one-dimensional Stefan problem for an "equivalent" spherical shell. We shall determine the interior radius of such ball, r_0, from the condition of equality of the focal spot area, πb^2, and the hemisphere area, $2\pi r_0^2$ ($r_0 = 2^{-1/2}b$); and the exterior radius from the condition of equality of the cylinder volume, $\pi a^2 l$, and half of the spherical shell volume, $2\pi(r_1^3-r_0^3)/3$ ($r_1=(r_0^3+ 3a^2l/2)^{1/3}$). Others ways of geometry recalculation are possible here.

In these assumptions $T=T(r,t)$ and the isothermal surface is a sphere $r=R(t)$. We introduce the following dimensionless variables and parameters:

$$r = r_1 x, \quad t = a_0^{-2} r_1^2 \tau, \quad T = T_w + (T_m - T_w)\theta, \quad a_0^2 = \lambda_L/(c_L\rho_L),$$
$$\lambda = \lambda_L \gamma(\theta), \quad c\rho = c_L\rho_L k(\theta), \quad h = \alpha r_1/\lambda_s, \quad p = Pc_L\rho_L(T_m - T_w),$$
$$Q(\theta) = q_0 - S(\theta)[1+L(\theta)], \quad qr_1 = q_0\lambda_L(T_m - T_w), \quad S(\theta) = S_k(\mu+\theta)^4,$$
$$S_k = \varepsilon\sigma r_1 (T_m - T_w)^3/\lambda_L, \quad \mu = T_w/(T_m - T_w), \quad Q_{EV}(T) = \varepsilon\sigma T^4 L(\theta),$$
$$X(\tau) = R(\tau)/r_1, \quad x_0 = r_0/r_1, \quad \gamma = \lambda_s/\lambda_L, \quad k = c_s\rho_s/(c_L\rho_L).$$

If we shall neglect by cooling from the surfaces being cooled then we shall obtained the one-dimensional Stefan problem

$$x^{-2}\frac{\partial}{\partial x}\left(x^2\gamma(\theta)\frac{\partial\theta}{\partial x}\right) - k(\theta)\frac{\partial\theta}{\partial\tau} - Px^2\dot{X}(\tau)\delta(x-X(\tau)) = 0, \quad x_0<x<1, \quad \tau>0,$$
$$\theta(x,0) = \varphi(x), \quad x_0<x<1, \quad \varphi(x_0) = 1; \qquad (1)$$

$$\frac{\partial\theta}{\partial x} = -Q(\theta), \quad x=x_0; \qquad \frac{\partial\theta}{\partial x} + h\theta = 0, \quad x=1, \ \tau>0; \qquad \theta(X(\tau),\tau) = 1.$$

Here the following notations were introduced: T_w is the water temperature in a cooling system, T_m is the melting temperature, $\lambda_L = const$, $\lambda_S = const$ are the thermal conductivity coefficients for liquid and solid phase respectively, $c_L = const$, $c_S = const$, $\rho_L = const$, $\rho_S = const$ are the specific heat and density for liquid and solid phase respectively, α is the coefficient of heat exchange with a contour being cooled by water; $p = \Lambda\rho_L$, Λ is the latent melting heat; q is the electron-beam heating power density being absorbed by the metal; ε, σ are the blackness degree and Stefan-Boltzmann constant; $Q_{ev}(T)$ is the heat flux density of evaporation; $\gamma(\theta) = \gamma + (1-\gamma)\eta(\theta-1)$, $k(\theta) = k + (1-k)\eta(\theta-1)$, $\eta(\theta)$ is the Heavyside function; S_k is the Stark coefficient; $\dot{X}(\tau) = dX/d\tau$; $\delta(x)$ is the Dirac function with the weight x^2; $\varphi(x)$ is an initial dimensionless temperature distribution being a result of evolution of a solution of the usual heat conduction problem (1) with $P=0$ and $\theta(x,0)=0$ to a moment τ_1 at which the metal surface $x=x_0$ is heated to the melting temperature $\theta(x_0,\tau_1)=1$ (this moment is taken as the zero of time).

At an electron beam power which is constant or monotonically increases up to some limiting value ($q(t)$ $q=const$) a steady state is established with the course of the time ($\theta(x,\tau)$ $\theta(x)$, $X(\tau)$ $x_s=const$). To determine it we obtain a stationary Stefan problem admitting the exact analytical solution

$$\theta(x) = \begin{cases} \theta_0 - x_0 Q(\theta_0)(1-x_0/x), & x_0 \le x \le x_s, \\ x_s F(x)/[F(x_s)x], & x_s \le x \le 1, \end{cases} \tag{2}$$

$$x_s = \frac{hx_0(\theta_0+\gamma-1)}{\gamma h + x_0(h-1)(\theta_0-1)}, \qquad Q(\theta_0) = \frac{h(\theta_0+\gamma-1)}{x_0 F(x_0)}, \tag{3}$$

where $F(y) = h + (1-h)y$, and $\theta_0 = \theta(x_0)$ is defined as an unique positive root of the equation $Q(\theta) + S(\theta)[1+L(\theta)] = q_0$.

From this solution we obtain practically important dependences of the melt volume, W, and the melt overheating, $\Delta T = \overline{T} - T_m$, ($\overline{T}$ is a mean temperature of the liquid metal) on input data, that is

on geometry, thermophysical parameters, intensity of the MEMS ($\tilde{k}=1/\gamma$), and electron beam power

$$W = 2\pi r_i^3 (x_*^3 - x_0^3), \tag{4}$$

$$\Delta T = \frac{x_0^2 (x_*^2 + x_0 x_* - 2x_0^2)}{2x_* (x_*^2 + x_0 x_* + x_0^2)} (T_m - T_H) Q(\theta_0). \tag{5}$$

A simple analysis shows that with an increase of the MEMS intensity the melt volume increases and the melt overheating decreases. Dependence of the heat flux density on the surface temperature θ_0 (q upon $T(r_0)$) sharply increases when the surface temperature achieves to a limiting value θ_0 mainly at the expense of an increase of the evaporation losses $S(\theta_0)L(\theta_0)$, therefore a further increase of the temperature θ_0 requires an unreasonably big increase of the electron beam power. Functional dependences obtained permit to find thermophysical characteristics λ_L, λ_S, α and the MEMS ratio $\tilde{k} = \lambda_L/\lambda_S$ using additional experimental information such as, for example, the melt volume, the melt overheating and the surface temperature of the liquid pool.

Technological singularities of the melting process require of obtaining of a determinate melt mass (of a liquid pool volume) with a preassigned overheating. Using of steady-state solution (2), (3) we can find basic melting parameters ensuring the obtaining of W and ΔT preassigned under the condition of a steady-state distribution of the metal temperature.

To this end we shall find θ_0 from the first formula (3)

$$\theta_0 = \left[\gamma h x_* - x_0 (\gamma h - F(x_*))\right] / \left[x_0 F(x_*)\right]. \tag{6}$$

Eliminating θ_0 with the help of (6) we obtain from the right side of the second equality (3)

$$Q(\theta_0) = h x_* / \left[\tilde{k} r_0^2 F(x_*)\right]. \tag{7}$$

Substituting (7) into (5) we find

$$\Delta T = \frac{h(x_*^3 + x_0 x_* - 2x_0^2)(T_m - T_H)}{2\tilde{k}(x_*^2 + x_0 x_* + x_0^2) F(x_*)},$$

from where

$$\tilde{k} = \frac{h(x_*^2 + x_0 x_* - 2x_0^2)(T_m - T_H)}{2\Delta T(x_*^2 + x_0 x_* + x_0^2)F(x_*)}. \qquad (8)$$

Taking into account that $Q(\theta_0) \equiv q_0 - S(\theta_0)[1 + L(\theta_0)]$, we have from (7)

$$q_0 = S(\theta_0)\left[1 + L(\theta_0)\right] + hx_*/\left[\tilde{k}x_0^2 F(x_*)\right]. \qquad (9)$$

Thus, the determination of the basic melting parameters (if the liquid pool volume W and melt overheating ΔT are given) we can conduct by the following scheme. For a known value of W we find from (4)

$$x_* = \frac{1}{(2\pi)^{1/3} r_1}(3W + 2\pi x_0^3 r_1^3)^{1/3},$$

later we determine $\tilde{k}$ with the help of (8), farther we obtain a value of θ_0 (6) and a value of q_0 from (9). With the help of q_0 we find the necessary heat flux power density of an electron beam

$$q = \tilde{k}\lambda_s(T_m - T_H)q_0/r_1.$$

The evolution of the temperature field $\theta(x,\tau)$ of the problem (1) is confined between a known initial distribution, $\theta(x,0) = 0$, and limiting steady-state one $\theta(x,\infty) = \theta(x)$. In addition we know a priori a monotone character of $\theta(x,\tau)$ dependences on x as well as on τ. This permits to take an approximate solution in the form (2) with constants θ_0 and x_* replaced by unknown functions $\theta_0(\tau)$ and $X(\tau)$

$$\theta(x,\tau) \approx \tilde{\theta}(x,\tau) = \begin{cases} \theta_0(\tau) - x_0 Q(\theta_0(\tau))(1 - x_0/x), & x_0 \le x \le X(\tau), \\ X(\tau)F(x)/[F(X(\tau))x], & X(\tau) \le x \le 1. \end{cases} \qquad (10)$$

If

$$X(\tau) = X(\theta_0) = \frac{x_0^2 F(x_0) Q(\theta_0(\tau))}{\gamma h + x_0(h-1)(\theta_0(\tau) - 1)}, \qquad (11)$$

then construction (10) satisfies the boundary conditions of the

problem (1) as well as the continuity condition for $x=X(\tau)$. Requiring the solution to satisfy the differential equation of an overall heat balance in the integral form

$$\int_{x_0}^{1}\left[\frac{\theta}{\partial x}\left(x^2\gamma(\tilde{\theta})\frac{\partial\tilde{\theta}}{\partial x}\right) - k(\tilde{\theta})\frac{\partial\tilde{\theta}}{\partial\tau}x^2\right]dx - PX^2(\tau)\dot{X}(\tau) = 0,$$

after computing the derivatives and integrals and eliminating of $\dot{X}(\tau)$ with the help of (11) we arrive to a Cauchy problem for $\theta_0(\tau)$

$$K(\theta_0)d\theta_0/d\tau = A(\theta_0) + BC(\theta_0), \quad \tau > 0, \quad \theta_0(0) = 1. \qquad (12)$$

Here

$$A(\theta_0) = x_0^2\left[Q(\theta_0) - h(\theta_{0\infty} + \gamma - 1)/[x_0F(x_0)]\right], \quad \theta_{0\infty} = \theta_0(\infty),$$

$$B = \gamma h^2/F(X_\infty), \quad x_* = X(\theta_{0\infty}), \quad C(\theta_0) = (x_* - X(\theta_0))/F(X(\theta_0)),$$

$$K(\theta_0) = X^2(\theta_0)M(X(\theta_0),\theta_0), \quad M(x,\theta) = P + \frac{kh[3h(1-x^3)+2(1-h)(1-x^3)]}{6x^3F^2(x)} +$$

$$+ \frac{2(x^3-x_0^3) - x_0(x_0+2x)(x-x_0)^2dQ(\theta)/d\theta}{6x^4[1 - x_0(1-x/x_0)dQ(\theta)/d\theta]}x_0^2Q(\theta).$$

The solution of the problem (12) is determined by the quadrature

$$\tau = \int_1^{\theta_0} K(\theta)/\left[A(\theta) + BC(\theta)\right]d\theta, \quad 1 \le \theta_0 \le \theta_{0\infty}. \qquad (13)$$

The idea to construct approximate solutions using "freed" parameters goes back to works by Leibenzon, Krylov, Bogolyubov and Mitropolsky.

The melting process in the model problem considered has a characteristic feature consisting in nearness of an asymptotic behavior of the solution for large values of τ to a logarithmic one. The first passage time of 95% of the steady-state value of the liquid pool surface temperature $\theta_{0\infty}$ is lesser than the corresponding first passage time of x_*. This corresponds to the thermophysical sense because the melting process is continued after the tem-

perature $\theta_0(\tau)$ attains of the almost limiting maximal value $\theta_{0\infty}$. Just as in the steady-state case, with intensifying of the MEMS there will be a decrease of the melt overheating and an increase of the melt volume.

To make dynamics of the melting process more precise, we have used a variational method essentially using a construction of an exact solution of the steady-state Stefan problem on every segment $x_{i-1}(\tau)\le x\le x_i(\tau)$ belonging to an arbitrary decomposition of the whole segment $x_0\le x\le 1$

$$\tilde{\theta}(x,\tau)=\theta_{i-1}(\tau)+\varphi_i(\tau)(x^{-1}-x_{i-1}^{-1}),\quad x_{i-1}(\tau)\le x\le x_i(\tau).$$

Boundary conditions, conditions of isothermality and continuity at the decompositions points $x=x_i(\tau)$ give a set of nonlinear equations, whereas conditions of the Bubnov-Galerkin method give a set of nonlinear ordinary differential equations for unknown functions $\theta_i(\tau)$, a coordinate of a melting isotherm $X(\tau)$, and auxiliary functions $\varphi_i(\tau)$. As a result the problem reduces to a Cauchy problem the solution of which is easily obtained using a computer by a numerical procedure. The computations accomplished for particular variants have shown the melt volume dynamics have well corresponded to the dynamics obtained on the basis of solution (10), (11) in the simplest case where the segment $x_0\le x\le 1$ have been decomposed into only two parts, $x_0\le x\le X(\tau)$ and $X(\tau)\le x\le 1$.

To estimate the obtained approximate analytical solutions we have also applied an implicit difference scheme with algebraic equations being linearized in every temporal "slice" of the Stefan problem for the isotherm field $x=x(\theta,\tau)$:

$$x^{-a}(\gamma(\theta)x^2/x_\theta)_\theta+k(\theta)x_\tau+Px_\tau(1,\tau)\delta(\theta-1)=0,\quad \theta_1(\tau)<\theta<\theta_0(\tau),\ \tau>0,$$

$$x(\theta,0)=x_0(\theta),\qquad \varphi(1)=\theta_1(0)\le\vartheta\le\theta_0(0)=1,$$

$$x(\theta_1(\tau),\tau)=1,\quad x(\theta_0(\tau),\tau)=x_0,\quad \tau>0, \tag{14}$$

$$1/x_\theta=-h\theta,\quad \theta=\theta_1(\tau);\qquad 1/x_\theta=-Q(\theta),\quad \theta=\theta_0(\tau),\quad \tau>0,$$

where $x_0(\theta)$ is the inverse function for $\varphi(x)$; $\theta_1(\tau)$ and $\theta_0(\tau)$ are minimum and maximum temperatures respectively to be found.

The passage from the Stefan problem (1) for the temperature field to the problem (14) for the isotherm field is realized with the help of the formulas of inverse functions differentiation and

the formula of the Dirac function transformation:

$$\theta_x = 1/x_\theta, \quad \theta_\tau = -x_\tau/x_\theta, \quad \partial/\partial x = x_\theta^{-1}\partial/\partial\theta; \quad x^2\delta(x-X) = \delta(\theta-1)/x_0.$$

This passage is competent provided that one-to-one correspondence between the coordinate x and the temperature θ for every time τ takes place. Here we have an existence and uniqueness theorem for the solution $x = x(\theta,\tau)$ under the condition that both an initial distribution $x_0(\theta)$ and the heat flux $Q(\theta)$ are monotonous.

In the formulation (14) it is necessary to determine the isotherm field $x(\theta,\tau)$ and the temperatures $\theta_1(\tau)$ and $\theta_0(\tau)$. Despite an apparent complication, the problem (14) proves to be more simple as regards a realization on the implicit difference scheme if it will be considered as a usual nonlinear conjugation problem with unknown moving boundaries being determined by additional conditions.

According to the problem's thermophysical sense, we know a minimum value θ_1 and a maximum one θ_0 of the dimensionless temperature. The first value is equal to a minimum value of the initial temperature and the second one is equal to a maximum value being attained in a steady-state regime. These values determine a constant segment of the dimensionless temperature's change containing the point $\theta=1$. All the intermediate intervals being corresponded to an arbitrary value of τ are contained in this segment evidently where $\theta_1(\tau)$ and $\theta_0(\tau)$ monotonously approaching at $\tau \to \infty$ to their limiting values attained in the steady state. This feature permits on a difference level to use uniform decompositions of the segments $[0,1]$ and $[1,\theta_0]$ into N^- and N^+ intervals respectively and to determine values of $\theta_1(\tau)$ and $\theta_0(\tau)$ at the nodes of such decompositions in the computation process. Then for $x_1(\theta)$ we obtain the set of the N^-+N^++1 nonlinear algebraic equations

$$x_1 = 1, \qquad x_{N^-+N^++1} = x_0,$$

$$\frac{\gamma}{x_{i+1}-x_i} - \frac{\gamma}{x_i-x_{i-1}} + \frac{2\gamma}{x_i} + \frac{k(x_i-\hat{x}_i)}{\Delta\tau} = 0, \quad 1 < i < i^*,$$

$$\frac{\gamma h^*}{x_{i+1}-x_i} - \frac{h^-}{x_i-x_{i-1}} + \frac{P(x_i-\hat{x}_i)}{\Delta\tau} = 0, \quad i = i^* = N^-,$$

$$\frac{1}{x_{i+1}-x_i} - \frac{1}{x_i-x_{i-1}} + \frac{2}{x_i} + \frac{x_i-\hat{x}_i}{\Delta\tau} = 0, \quad i^* < i < N^- + N^* + 1,$$

where the superscript "^" denotes a value corresponding to the preceding temporal slice.

Linearizing this set with the help of the equations

$$(x^{s+1} - y^{s+1})^{-1} \approx 2(x^s + y^s)^{-1} - (x^{s+1} - y^{s+1})(x^s - y^s)^{-2},$$

where the index "s" indicates an order of iteration in the temporal slice considered, one can obtain the three-diagonal set of the equations

$$A_i x_{i+1}^{s+1} + B_i x_i^{s+1} + C_i x_{i-1}^{s+1} = F_i, \quad i = 1, N^- + N^* + 1.$$

Here

$$A_i = 0, \quad B_i = 1, \quad C_i = 0, \quad F_i = 1, \quad i = 1;$$

$$A_i = \gamma h_{i+1}^2, \quad B_i = \gamma(2\nu^2 - h_{i+1}^2 - h_i^2 - k\eta), \quad C_i = \gamma h_i^2, \quad F_i = 2\gamma(h_{i+1} - h_i + 2\nu - k\hat{x}_i\eta), \quad 1 < i < i^*;$$

$$A_i = -h^* h_{i+1}^2, \quad B_i = \gamma h^* h_{i+1}^2 + \gamma h_i^2 h^- + P\eta, \quad C_i = -\gamma h^- h_i^2, \quad F_i = P\hat{x}_i\eta - 2\gamma h^* h_{i+1} + 2\gamma h^- h_i, \quad i = i^*;$$

$$A_i = h_{i+1}^2, \quad B_i = 2\nu - h_{i+1}^2 - h_i^2 - \eta, \quad C_i = h_i^2, \quad F_i = 2(h_{i+1} - h_i + 2\nu) - \hat{x}_i\eta, \quad i^* < i < N^- + N^* + 1;$$

$$A_i = 1, \quad B_i = 0, \quad C_i = 0, \quad F_i = x_0, \quad i = N;$$

$$h_i = (x_i^s - x_{i-1}^s)^{-1}, \quad h^- = 1/N^-, \quad h^* = (\theta_0 - 1)/N^*, \quad \nu = 1/x_1^s, \quad \eta = 1/\Delta\tau.$$

A peculiarity of these sets is connected with the number of the equations in each s-th temporal slice. In the process of their solving by the sweep method, the additional conditions

$$1/x_\theta = -h\theta, \quad \theta = \theta_1(\tau); \qquad 1/x_\theta = -Q(\theta), \quad \theta = \theta_0(\tau). \tag{15}$$

should be checked. If these are satisfied, or rather inequalities following from them are satisfied, going over to the next temporal slice may be performed. Otherwise the number of the equations is

changed, namely, it is increased by 1 if the second condition (15) is violated or decreased by 1 if the first one in (15) is violated. The numerical computations for particular problems have shown there has been a computational stability if the number of the decomposition points with respect to θ has been doubled under the condition of the equality of the minimum step (h^- or h^+) of θ and a step of the time τ. The question how to choose a relation between $\Delta\tau$ and $h=\Delta\theta$ remains open. According to the physical meaning of the problem, with good reason one may assume that the optimal choice would be the equality of the steps. An analysis of the computations performed has permitted to trace a stabilization of temperature fields as well as isotherm fields to limiting steady states. A comparison has shown times of nearly complete attainment of the steady state (95%) computed using formula (13) with $\theta_0 = 0.95\theta_{0\infty}$ and by a selection from results of difference scheme computations are practically equal. The fields $x=x(\theta,\tau)$, $\theta=\theta(x_0,\tau)$ are also coordinated satisfactorily with the approximate analytical solutions obtained.

It is quite naturally that a tabular information about solutions obtained with the help of a difference scheme is considerably poorer in comparison with an analytical one with respect to functional dependences between basic and input parameters of the melting process, solution of inverse problems, prediction and optimization needed for engineering practice. In the same time results of numerical computations permit to evaluate an error of approximate analytical solutions which as a rule cannot be evaluated analytically. The computations performed have shown the approximate analytical solutions obtained may be refined no more than 5-10%.

3. MATHEMATICAL MODELS WITH TWO SPACE VARIABLES

More exact and more complicated mathematical models are two-dimensional axisymmetric ones. One may consider these mathematical models essentially correspond adequately to the thermophysical model of the vacuum EBAM in an cylindrical autocrucible with the lateral surface $r=a$ and the bottom surface $z=0$ being cooled whereas on the top surface $z=l$ kinetic energy 20-40 keV electrons

flux is converted into heat energy with the density $q = q(r,t)$. The temperature field of the cylinder being heated is axisymmetric and its determination requires of solving the nonlinear equation

$$r^{-1}\frac{\partial}{\partial r}\left(r\lambda(T)\frac{\partial T}{\partial r}\right) + \frac{\partial}{\partial z}\left(\lambda(T)\frac{\partial T}{\partial z}\right) = \gamma(T)\frac{\partial T}{\partial t} +$$

$$+ \rho r R_t(z,t)\delta(r-R(z,t)), \quad 0<r<a, \quad 0<z<l, \quad t>0;$$

with the initial condition

$$T(r,z,0) = T^0(r,z)$$

and the boundary conditions

$$\frac{\partial T}{\partial r} = 0, \quad r = 0; \qquad \lambda_s(T)\frac{\partial T}{\partial r} + \alpha_1(z)(T-T_w)=0, \quad r = a;$$

$$\lambda_s(T)\frac{\partial T}{\partial z} - \alpha_2(r)(T-T_w)=0, \ z=0; \quad \lambda(T)\frac{\partial T}{\partial z} = q(r,t)-f(T), \quad z = l,$$

as well as the condition on an isothermal melting surface $r=R(z,t)$

$$T(R(z,t),z,t)=T_m.$$

Here $\gamma(T)=c(T)\rho(T)$,

$$\omega(T)= \begin{cases} \omega_s(T), & T < T_m, \\ \omega_L(T), & T \geq T_m, \end{cases} \qquad \omega = \lambda;\ c;\ \rho;$$

$f(T)=\varepsilon\sigma T^4+ \eta(T-T_m)Q_{ev}(T)$ is the flux density of heat losses at the expense of radiation and evaporation from the surface $z=l$ being heated ($\eta(T)$ is the Heavyside function); in the general case the coefficients of heat exchange on the surfaces being cooled $\alpha_1(z)$, $\alpha_2(r)$ may be functions of z, r respectively.

According to a thermophysical meaning of the problem, there would be a stabilization to a limiting steady state if overall supplied heat flux is completely balanced by means of the cooling system and by heat losses connected with radiation and evaporation. The steady-state equations of heat conduction and the boundary conditions are written in the form

$$\frac{1}{r}\frac{\partial}{\partial r}\left(\lambda_i(T)r\frac{\partial T}{\partial r}\right) + \frac{\partial}{\partial z}\left(\lambda_i(T)\frac{\partial T}{\partial z}\right) = 0, \quad (r,z)\in \Omega_i, \quad i=S,L;$$

$$\frac{\partial T}{\partial r} = 0, \quad r = 0; \qquad \lambda_s(T)\frac{\partial T}{\partial r} + \alpha_1(z)(T - T_w) = 0, \quad r = a; \tag{16}$$

$$\lambda_s(T)\frac{\partial T}{\partial z} - \alpha_2(r)(T - T_w) = 0, \quad z = 0; \qquad \lambda(T)\frac{\partial T}{\partial z} = q(r) - f(T), \quad z = l.$$

Here the domain $\Omega = \{ (r,z): 0<r<a; 0<z<l \}$ is divided by the solid-liquid boundary into two subdomains $\Omega_s = \{ (r,z) \in \Omega: T(r,z) < T_m \}$ and $\Omega_L = \{ (r,z) \in \Omega: T(r,z) > T_m \}$, being corresponded to the solid and liquid phase of metal.

On an unknown solid-liquid interface $r = R(z)$ the equality conditions of the metal temperature and the melting temperature as well as of the heat fluxes from the sides of the liquid and solid phases in the steady state must be fulfilled

$$T(R(z),z) = T_m; \qquad \lambda_L \frac{\partial T}{\partial n}\bigg|_{r=R(z)-0} = \lambda_s \frac{\partial T}{\partial n}\bigg|_{r=R(z)+0}. \tag{17}$$

We shall use the well-known hypothesis that forced convective heat transfer in the melt conditioned by the MFMS may be imitated with the help of the coefficient of effective thermal conductivity, $\lambda_E = \tilde{k}\lambda_L$, where λ_L is the coefficient of molecular thermal conductivity. To determine a value of $\tilde{k}$ one may use the formula obtained as a result of experimental investigations of turbulent heat transfer in the case of forced convection [9]:

$$\tilde{k} = \begin{cases} 0.45(PrRe)^{0.438} & \text{при } PrRe \le 8600; \\ 1.35 \cdot 10^{-5}(PrRe)^{1.84} & \text{при } PrRe > 8600. \end{cases} \tag{18}$$

Taking into account that $PrRe = 2v_m r_* C_{vL}/\lambda_L$, we see $\tilde{k}$ depends on the heat capacity of the unit of the liquid metal volume C_{vL} and a mean melt motion velocity v_m as well as on a mean pool radius r_*. In the work [10] one used in calculations the value $\tilde{k} = 10$ for the case where electromagnetic stirring was sufficiently intense.

Assuming the coefficient of effective thermal conductivity $\lambda_E = const$ in the liquid phase domain, $\alpha_1(z) = \alpha_1 = const$, $\alpha_2(r) = \alpha_2 = const$, the steady-state Stefan problem (16), (17) is transformed to the form

$$\frac{1}{r}\frac{\partial}{\partial r}\left[\lambda(T) r \frac{\partial T}{\partial r}\right] + \frac{\partial}{\partial z}\left[\lambda(T)\frac{\partial T}{\partial z}\right] = 0, \qquad (r,z) \in \Omega_s;$$

$$\frac{1}{r}\frac{\partial}{\partial r}\left(r\frac{\partial T}{\partial r}\right)+\frac{\partial^2 T}{\partial z^2}=0,\qquad (r,z)\in\Omega_L;$$

$$\frac{\partial T}{\partial r}=0,\quad r=0;\qquad \lambda(T)\frac{\partial T}{\partial r}+\alpha_1 T=\alpha_1 T_w,\quad r=a;\qquad (19)$$

$$\lambda(T)\frac{\partial T}{\partial z}-\alpha_2 T=-\alpha_2 T_w,\quad z=0;\qquad \lambda(T)\frac{\partial T}{\partial z}=q(r)-f(T),\quad z=l;$$

$$T=T_m,\quad r=R(z);\qquad \lambda_s\frac{\partial T}{\partial n}\Big|_{r=R(z)-0}=\lambda(T)\frac{\partial T}{\partial n}\Big|_{r=R(z)+0}$$

We shall represent the function $Q_{sv}(T)$ designating the density of the heat flux of evaporation in the form $Q_{sv}(T)=c_1 exp(-c_2/T)$ where one may find the parameters c_1, c_2 using both experimental investigations data and the Clapeyron-Klausius law written for a thin gas layer closely approximating to the evaporation surface, [11,12].

To reduce the problem (19) to an equivalent nonlinear integral equation we apply the Kirchhoff transformation

$$u(T)=\int_0^{T-T_w}\lambda(\tau)d\tau.$$

If to approximate a dependence of the thermal conductivity coefficient on the temperature by the step function

$$\lambda(T)=\lambda_i,\ T_{i-1}\le T<T_i,\ i=\overline{1,K};\ (T_K=T_m,\ T_0=T_w);\quad \lambda(T)=\tilde{k}\lambda_L,\ T>T_m;$$

or by the linear dependence in the solid phase domain

$$\lambda_s(T)=\lambda_s(T_0)+\beta(T-T_0),\ T_0\le T\le T_m;\quad (T_0=T_w);\quad \lambda(T)=\tilde{k}\lambda_L,\ T>T_m,$$

we can find the inverse function $T(u)$ in an analytical form.

If we exclude $T(r,z)$, from (19) we obtain the simpler boundary problem for a new unknown function, $u(r,z)$.

$$\frac{1}{r}\frac{\partial}{\partial r}\left(r\frac{\partial u}{\partial r}\right)+\frac{\partial^2 u}{\partial z^2}=0,\ 0<r<a,\ 0<z<l;\quad \frac{\partial u}{\partial r}+h_1 u=0,\ r=a;\qquad (20)$$

$$\frac{\partial u}{\partial r}=0,\ r=0;\quad \frac{\partial u}{\partial z}-h_2 u=0,\ z=0;\quad \frac{\partial u}{\partial z}=q(r)-f(T(u)),\ z=l$$

and the condition for the determination of an interface $r=R(z)$ between the solid and liquid phases

$$u(R(z),z) = u_m. \qquad (21)$$

Here $h_i=\alpha_i/\lambda_{si}$, $i=1,2$; where λ_{si} are mean values of λ_s on the surfaces $r=a$ and $z=0$ respectively; $u_m = u(T_m)$.

We shall consider Green's function, $G(r,z;\rho,\eta)$, determined as a solution of the linear boundary problem with the homogeneous boundary conditions

$$\frac{1}{r}\frac{\partial}{\partial r}\left(r\frac{\partial G}{\partial r}\right) + \frac{\partial^2 G}{\partial z^2} = -\delta(r-\rho)\delta(z-\eta),$$

$$0 < r,\rho < a, \quad 0 < z,\eta < l;$$

$$\frac{\partial G(0,z;\rho,\eta)}{\partial r} = 0, \qquad \frac{\partial G(a,z;\rho,\eta)}{\partial r} + h_1 G(a,z;\rho,\eta) = 0;$$

$$\frac{\partial G(r,0;\rho,\eta)}{\partial z} - h_2 G(r,0;\rho,\eta) = 0; \qquad \frac{\partial G(r,l;\rho,\eta)}{\partial z} = 0,$$

where the formal relations for the Dirac function take place

$$\int_0^l g_1(z)\delta(z-\eta)dz = g_1(\eta), \qquad \int_0^a g_2(r)\delta(r-\rho)rdr = g_2(\rho).$$

The Green function is found in the form

$$G(r,z;\rho,\eta) = \frac{2}{a^2}\sum_{n=1}^{\infty} \frac{\gamma_n J_0(\gamma_n\rho)\, J_0(\gamma_n r)\, g_n(z,\eta)}{(h_1^2+\gamma_n^2)[\gamma_n sh(\gamma_n l) + h_2 ch(\gamma_n l)]J_0^2(\gamma_n a)},$$

where $g_n(z,\eta) = [\gamma_n ch(\gamma_n z) + h_2 sh(\gamma_n z)]ch(\gamma_n(l-\eta))$, $z\le\eta$; $g_n(\eta,z) = g_n(z,\eta)$; $\gamma_n>0$ are roots of the equation $h_1 J_0(\gamma a) - \gamma J_1(\gamma a) = 0$; $J_n(z)$ are the Bessel function of the first kind and n-th order.

The problem (20) is reduced to an equivalent nonlinear integral equation

$$u(r,z) = u_0(r,z) - \int_0^a G(r,z;\rho,l)f(T(u(\rho,l)))\rho d\rho, \qquad (22)$$

where

$$u_0(r,z) = \int_0^a q(\rho)G(r,z;\rho,l)\rho d\rho.$$

Substituting $z=l$ into (22) we arrive to the nonlinear integral Hammerstein equation for determining the function $v(r)=u(r,l)$

$$v(r) = v_0(r) - \int_0^a G(r,\rho) f[T(v(\rho))]\rho d\rho, \qquad (23)$$

where $v_0(r)=u_0(r,l)$, $G(r,\rho)=G(r,l;\rho,l)$. After solving integral equation (23) the function $u(r,z)$ and the solid-liquid interface $r=R(z)$ are found from quadrature (22) and equation (21) respectively.

To find an approximate solution of equation (23) we approximate $v(r)$ by the step function and designating a mean integral value of $v(r)$ on the interval (r_{i-1},r_i) by v_i, where r_i are decomposition points of the segment $[0,a]$ into M parts. After applying the variational method we obtain the system of the nonlinear equations for determining of v_j, $j=\overline{1,M}$.

$$v_j = v_{0j} - \sum_{i=1}^{M} G_{ij} f(T(v_i)), \quad j = \overline{1,M}; \qquad (24)$$

where the constants v_{0j}, G_{ij} are found by the integration of known functions.

After finding of v_j, $j=\overline{1,M}$, we can represent the modified temperature in the form of a series

$$u(r,z) = \frac{2}{a^2} \sum_{n=1}^{\infty} A_n(z) J_0(\gamma_n r), \qquad (25)$$

where $A_n(z)=\left[\gamma_n \int_0^a rq(r)J_0(\gamma_n r)dr/4P_n - \sum_{i=1}^{M} f(T(v_i))A_{ni}\right]g_n(z)$; $A_{ni}=[r_i \times$

$\times J_1(\gamma_n r_i)-r_{i-1}J_1(\gamma_n r_{i-1})]/P_n$; $P_n=(\gamma_n^2+h_1^2)[\gamma_n+h_2-(\gamma_n-h_2)exp(-2\gamma_n l)]\times$

$\times J_0^2(\gamma_n a)$; $g_n(z)=(\gamma_n+h_2)exp(-\gamma_n(l-z))+(\gamma_n-h_2)exp(-\gamma_n(l+z))$.

Using a simplified approach we can assume the coefficient of effective thermal conductivity is a known number ($\lambda_e=const$) independent of a solution of the heat conduction problem. In that case it remains to solve system (24).

Using an other approach where a value of $\lambda_e=\tilde{k}\lambda_L$ is determined in the course of solving of the problem we can use formula (28) according to which $\tilde{k}$ depends on a mean melt stirring velocity v_m and a mean radius of the liquid pool, r_*. We shall assume the value of v_m is determined by the action intensity of the MEMS system

only. If the value of v_m is given the determination of $\tilde{k}$ is reduced to finding of a mean integral value of the liquid pool radius

$$r_m = \int_{z_0}^{l} R(z)dz/(l-z_0) \qquad (26)$$

over its depth, $H=l-z_0$, is also to be determined. Here z_0 is a solution of the equation $R(z)=0$. In this case it is impossible to find a solution of system (24) because the parameter $\tilde{k}$ is used for determining of a relation between the functions T and u.

Let us describe of the solving procedure of the problem in this case. Evidently we can find $\tilde{k}=\tilde{k}(r_m)$ from (18) and compute $\lambda_E=\tilde{k}(r_m)\lambda_L$ for every value of $r_m \in (0,a)$ and later we can solve system (24). Further considering equation (21) for a sequence of discrete values of z_i we can find a sequence of corresponding values of the function $r_i=R(z_i)$ with the help of which we can compute the right side of equality (26). Thus we can write relation (26) in the form

$$r_m = \Psi(r_m), \qquad (27)$$

where $\Psi(r_m)$ is a function which for every $r_m \in (0,a)$ correlates a computation result of the right side of (26) obtained in the way stated above. Thus, the determination of a mean integral value of the pool radius r_m is practically reduced to the numerical solving of functional equation (27) by an iterative procedure.

Thus, after finding an approximate solution of equation (27) we can find a coefficient of effective thermal conductivity $\lambda_E=\tilde{k}(r_m)\lambda_L$, a modified temperature field $u(r,z)$ and a solid-liquid boundary $r=R(z)$ a mean integral value of the radius of which is equal to r_m. The desired steady-state temperature field $T(r,z)$ is determined by the inversion of the Kirchhoff transformation $u(T)$.

The liquid pool volume W, the mean integral melt overheating over the whole pool volume ΔT and the melt overheating on the pool surface ΔT_l are computed by means of the formulas

$$W = \pi \int_{z_0}^{l} R^2(z)dz, \qquad \Delta T = \frac{2\pi}{W} \int_{z_0}^{l} \int_{0}^{R(z)} T(r,z)rdrdz - T_m.$$

$$\Delta T_l = \frac{2}{R^2(l)} \int_0^{R(l)} T(r,l) r dr - T_m .$$

In practice of the EBAM the heating is realized by an focused electron beam scanning over the surface being heated according to a given program (a circle, a spiral, intersecting lines and others).

Let us determine $q(r)$ that is a steady-state distribution of the power density on the heating surface in the case of the scan of an electron beam over the circle of radius $0<R<a$. Let O_1 is a focusing point of a beam situated on the plane $z=l$ and $|OO_1|=R$, where O is situated on the same plane in the autocrucible axis. Let consider a point $M(\beta)$ a distance from which to the point O is equal to r and one to the point O_1 is equal to $y(\beta)$, where $\beta=\angle O_1OM(\beta)$. At the point $M(\beta)$ a value of the power density is equal to $q_0 \exp[-k_r y^2(\beta)]$ where $y^2(\beta)=R^2+r^2-2rR\cos\beta$, $0\le\beta\le\pi$ (from the cosine theorem), $q_0 = Pk_r/\pi$ is a value of the heating power density in the focusing point of a beam, P is the heating power being absorbed by the metal, $k_r=2b^{-2}$ is a concentration coefficient of the heat source in the radial direction, b is a focal spot radius. Density of the energy being absorbed at every point a distance from which to the point O is equal to r at time when the electron beam passes the one whole circle of radius R (in the rotation period $T_{sc}=2\pi R/v_{sc}$, where v_{sc} is a scan velocity) is determined by the integral

$$E(r) = 2q_0 \int_0^{T_{sc}/2} \exp(-k_r[r^2+R^2-2Rr\cos(v_{sc}t/R)])dt =$$

$$= \frac{2Rq_0}{v_{sc}} \exp[-k_r(r^2+R^2)] \int_0^{\pi} \exp(2k_r rR\cos\beta)d\beta .$$

As $q(r)$ we accept a mean value of the energy density being absorbed per unit time

$$q(r) = \frac{E(r)}{T_{sc}} = \frac{q_0}{\pi} \exp[-k_r(r^2+R^2)] \int_0^{\pi} \exp(2k_r rR\cos\beta)d\beta . \qquad (28)$$

From (28) for $R=0$ we obtain the known formula of the normal

distribution $q(r)$ in the case of the axisymmetric heating by a fixed beam: $q(r)=q_0 exp(-k_r r^2)$.

If we expand the exponential function in (28) in the form of a Taylor series the expression of $q(r)$ can be written as

$$q(r) = q_0 exp[-k_r(r^2+R^2)]\left[1 + \sum_{n=1}^{\infty} \frac{(2n-1)!!}{(2n)!!} \frac{(2k_r rR)^{2n}}{(2n)!}\right].$$

The investigation of the function $q(r)$ from (28) apropos an extremum shows that a maximum point of $q(r)$, $r=r_0$, is determined by the equation

$$\int_0^{\pi} (R\cos\beta - r)exp(2k_r rR\cos\beta)d\beta = 0, \qquad (29)$$

from which we obtain the inequalities $0\le r_0<R$. These inequalities are verified by a form of the curves $q(r)/q_0$ which are shown in Fig.2 for the case where $b=0.03$ m and the scan radius R takes various values: 1 - $R=0$; 2 - $R=0.015$ m; 3 - $R=0.025$ m; 4 - $R=0.03$ m; 5 - $R=0.04$ m; 6 - $R=0.5$ m. If $R=0$ and $R=0.15$ m then a maximum point $r_0=0$ but if R is further increased then maximum points are situated in the interval $(0,R)$. Thus, for specific values of R the trajectory (a circle) of a maximum absorption of the heating energy is situated interior to the circle bounded by the scan trajectory $r=R$ but not on the line $r=R$ of the beam focusing. Equation (29) can be written as

$$1 + \sum_{n=1}^{\infty} \frac{(2n-1)!!}{(2n)!!}\left[\frac{2k_r r^2}{(2n)!} - \frac{1}{(2n-1)!}\right](2k_r)^{2n-1}R^{2n}r^{2n-2} = 0.$$

Restricting ourselves by two terms of the series we obtain the biquadratic equation

$$k_r^4R^4r^4 + 2k_r^2R^2(2 - k_rR^2)r^2 - 4(k_rR^2 - 1) = 0,$$

from which we find the approximate value of r_0:

$$r_0 \approx [2(k_rR^2 - 1)]^{1/2}/(k_rR),$$

and the condition for $r_0>0$

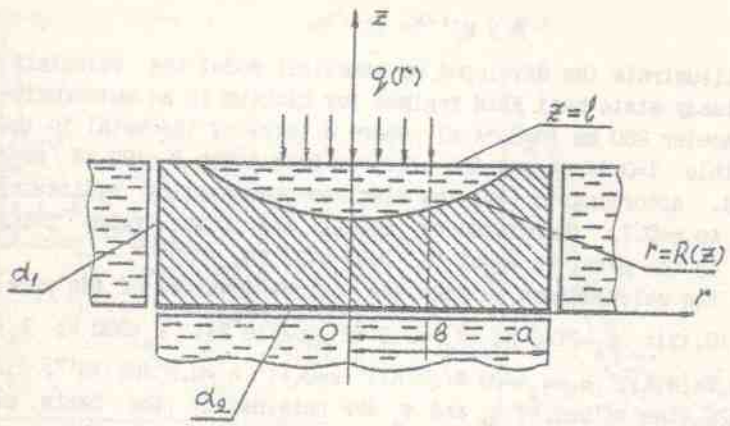

Fig. 1

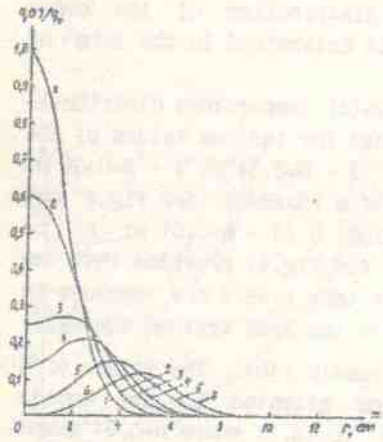

Fig.2

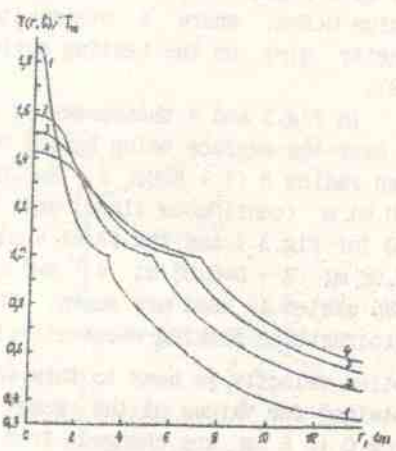

Fig.3

$$R > k_r^{-1/2} = 2^{-1/2} b.$$

To illustrate the developed mathematical model the calculations of steady-state heat EBAM regimes for niobium in an autocrucible of diameter 280 mm (a=0.14 m) where a level of the metal in the autocrucible l=0.14 m and the electron beam power P_0=190 kW were performed. According to [10] the electron-beam heating efficiency is equal to η=0.7, therefore we accept the power value being absorbed by the metal is equal to $P=\eta P_0$=133 kW.

For the calculations we take the following values of the parameters [10,13]: T_m=2740 K; C_{vL}=0.2772·10^{7}J/(m^{3}K); T_w=300 K; λ_L= =56.2716 W/(M·K); $\alpha_1=\alpha_2$=400 W/(m^{2}K); ε=0.4; c_1=0,31102·10^{18}; c_2= =93868.526 (the values of c_1 and c_2 are obtained of the basis of the experimental data from [1]). In the solid phase domain we consider a step dependence of the thermal conductivity coefficient on the temperature obtained with the help of data [13] about the niobium heat conductivity. We consider an axisymmetric heating of metal by a fixed (R=0) or scanning electron beam over the circle of radius $0<R<a$, where a steady-state distribution of the power density $q(r)$ on the heating surface is determined in the form of (28).

In Fig.3 and 4 the curves of the metal temperature distribution over the surface being heated obtained for various values of the scan radius R (1 - R=0; 2 - R=0.02 m; 3 - R=0.04 m; 4 - R=0.06 m; b=0.01 m (continuous lines) and b=0.04 m (dashed) for Fig.4 and R=0 for Fig.3) and the focal spot radius b (1 - b=0.01 m; 2 - b= =0.02 m; 3 - b=0.03 m; 4 - b=0.04 m for Fig.4) provided that the MEMS system is used are shown. Here we take v_m=0.3 m/s because in autocrucibles working substantively with the MEMS systems the metal motion velocity is near to this value namely [10]. The values of $\tilde{k}$ obtained for values of the scan radius situated in the bounds from 0 to 6 cm are changed from 8.34 to 13.11 where b=0.01 m and from 11.79 to 12.88 for b=0.04 m that is these values are near to the value $\tilde{k}$=10 [10]. A comparison of the curves of the melt surface temperature obtained for b=0.03 m, v_m= 0.3 m/s (continuous

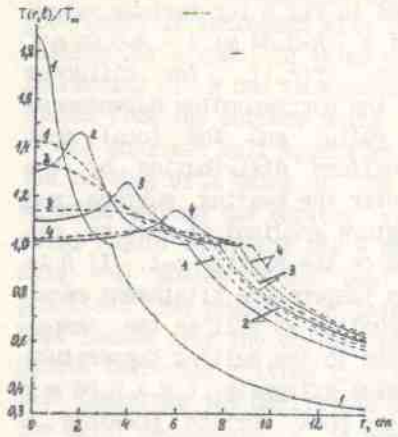

Fig.4

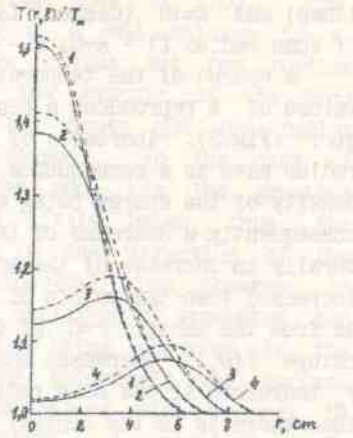

Fig.5

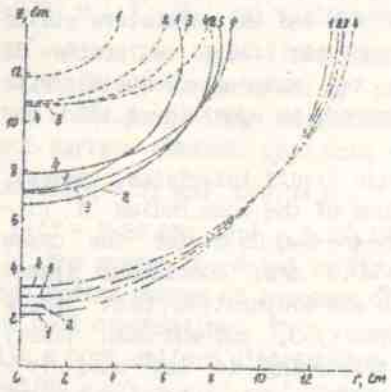

Fig.6

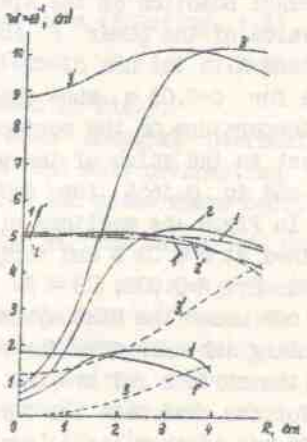

Fig.7

lines) and $\tilde{k}=10$ (dashed) is presented in Fig.5 for various values of scan radius (1 - $R=0$; 2 - $R=0.02$ m; 3 - $R=0.04$ m; 4 - $R=0.06$ m).

A course of the temperature curves $T(r,l)$ for different values of R reproduces a behavior of the corresponding dependences $q(r)$ (Fig.2). Increases of the scan radius and the focal spot radius have as a consequence a more uniform distribution of the density of the energy being absorbed over the heating surface and consequently a decrease of the temperature gradient as well as naturally an increase of the pool radius on the surface $z=l$. If R is increased then the points of a maximum temperature attainment recede from the center $r=0$ of the pool surface as well as the temperature $T(0,l)$ decreases and approaches to the melting temperature T_m therefore if the scan radius increases extremely ($R > 0{,}06$ м) then there is in the central part of the pool surface possible a formation of a solid metal zone. Going over the melting temperature the temperature curves have a break point. This is stipulated by a distinction of the thermal conductivity coefficients for the melt and solid metal.

To determine the error admitted by approximate solving of nonlinear boundary problem (20) we have computed the value of the summary energy losses from the surfaces $z=l$, $z=0$ and $r=a$ which for the exact solution of the steady-state problem must be the same as the value of the power P absorbed by the metal. The calculations realized with the use of the niobium data and the parameters stated above for $b=0.03$ m show that the error admitted to determine of the temperature on the surfaces $z=l$, $z=0$ and $r=a$ computed with respect to the value of the power absorbed is equal to 1.36% for $R=0$ and to 0.165% for $R=0.03$ m.

In Fig.6 the sections of the solid-liquid interfaces, $r=R(z)$, obtained at $b=0.03$ m and various values of the scan radius R (1 - $R=0$; 2 - $R=0.03$m; 3 - $R=0.04$ m; 4 - $R=0.05$ m) for the cases when one uses the MEMS system ($v_m=0.3$ m/s, continuous lines) including the case when the radiation and evaporation heat losses from the surface $z=l$ are not considered ($f=0$, dot-and-dash lines) and for the case when the forced melt stirring is not used ($v_m=0.005$ m/s, dashed lines) are presented. In this last case for the variation of the scan radius from 0 to the value $R=0.05$ m the

value of $\tilde{k}$ is changed in the bounds from 1.44 to 2.00. The pool depth is increased with increasing of R and achieves to a maximum for a specific value of the scan radius but for further increasing of R one is decreased. At the expense of the heat losses from the surface being heated the depth and the radius of the pool are half approximately decreased. In the case of the melting with using of the MEMS the pool has the greatest diameter not on the surface $z=l$ but a little below, thus, the solid-liquid interface has a small bend in the direction of the axis $r=0$ adding to the pool an ellipsoidal form observed in practice. The presence of this bend is explained by exceeding the heat losses over the energy density values being absorbed in the points where the melting isotherm surface intersects the surface $z=l$ therefore the derivative of the temperature with respect to the axial coordinate, z, is near the surface $z=l$ negative. In the two other cases this derivative is positive ($v_m=0.005$ m/s) and one is equal to zero ($f=0$). It will be noted that in the case of the linear problem ($f=0$) a disposition of the solid-liquid phase boundary $r=R(z)$ becomes independent of the effective thermal conductivity coefficient.

Dependences of niobium liquid pool volume upon scan radius for the cases where $v_m=0.3$ m/s (continuous lines), $v_m=0.005$ m/s (dashed) and $f=0$ (dot-and-dash) for $b=0.01$ m (indexing 1-3) and $b=0.04$ m ($1'-3'$) and various values of power P ($1;1'$- $P=65$ kW; $2;2'$- $P=100$ kW; $3;3'$ - $P=133$ kW) are shown in Fig.7.

In Fig.8 dependences of niobium mean integral overheating over whole pool volume (continuous lines) and melt overheating on pool surface (dashed) upon scan radius for the cases where $b=0.01$ m (indexing 1-3) and $b=0.04$ m ($1'-3'$) for various values of power P ($1;1'$- $P=65$ kW; $2;2'$- $P=100$ kW; $3;3'$ - $P=133$ kW) are presented.

The graphs presented in Fig.7,8 show that an increase of the scan radius causes an increase of the pool volume and a decrease of the melt overheating. This is completely explained in connection with a more uniform distribution of the energy absorbed over the heating surface with an increase of R. But in the case of the melting with the MEMS an extreme increase of the scan radius causes

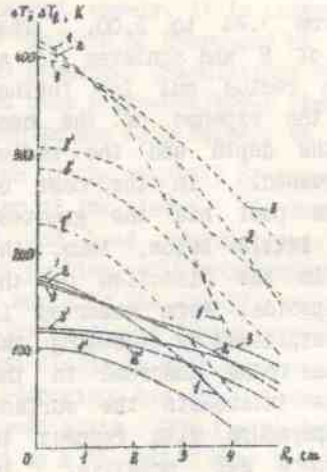

Fig.8

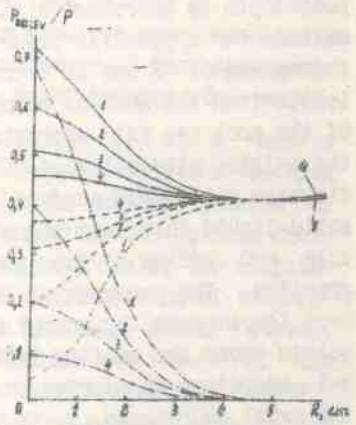

Fig.9

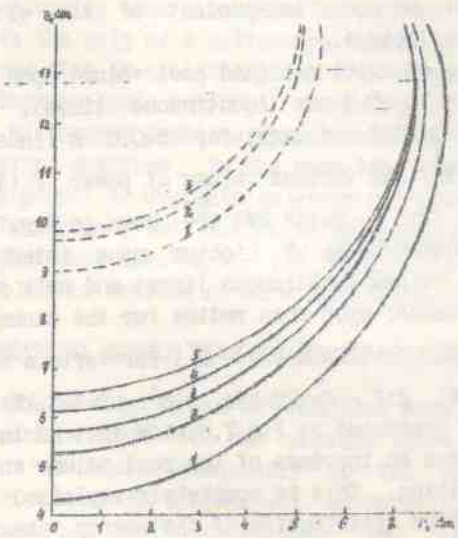

Fig. 10

a decrease of the volume end for every b the dependence $W(R)$ has an attainment point of a maximum. A comparison of the curves $W(R)$ obtained for v_m=0.005 m/s and v_m=0.3 m/s shows that the use of the MEMS permits to obtain for R=0 the volume which is 7.5-20 times bigger (depending on a value of b) and for R=5 cm, for example, 2.8-3.5 times bigger. Applying the circular scan of the electron beam the pool volume for b=1 cm can be obtained 12 times bigger (in comparison with the axisymmetric heating by a fixed beam) and for b=4 cm the volume is increased by 15%. At the expense of the heat losses from the surface being heated the liquid pool volume is 2.5-4 times decreased for the power being absorbed P=65-133 kW. The melt overheating on the pool surface is more than 2 times bigger than the mean integral overheating over the whole pool volume (Fig.8).

In Fig.9 dependences of the relative summary energy losses by radiation and evaporation from the heating surface, P_{RD+EV}/P, (continuous lines), the losses by radiation, P_{RD}/P, (dashed lines) and by metal evaporation, P_{EV}/P, (dot-and-dash ones) on the scan radius R for $\tilde{R}$=10 and various values of the focal spot radius (1 - b=0.01 m; 2 - b=0.02 m; 3 - b=0.03 m; 4 - b=0.04 m) are shown. An analysis permits to conclude that with an increase of the scan radius the summary losses P_{RD+EV} are decreased, the contribution of the radiation losses is increased and one of evaporation is decreased. Let us give attention to the fact of a stabilization of the summary losses and the presence of a minimum value of P_{RD+EV}/P for a specific value of the scan radius (a maximum value of the liquid pool volume corresponds to which (Fig.7)). This points to possibility of principle of such construction of the EBAM technological process for which the energy losses by means of radiation and evaporation may be reduced to a minimum.

At the reduction of Stefan problem (19) to problem (20) for the modified temperature $u(r,z)$ a dependence of the thermal conductivity coefficient $\lambda_s(T)$ on temperature on the surfaces r=a and z=0 is not taken into account but constant (mean) values of λ_s are utilized. After an application of the Kirchhoff transformation to the more complicated problem (16), (17) we obtain the nonlinear boundary problem for determination of $u(r,z)$

$$\frac{1}{r}\frac{\partial}{\partial r}\left(r\frac{\partial u}{\partial r}\right)+\frac{\partial^2 u}{\partial z^2}=0,\quad 0<r<a,\ 0<z<l;$$

$$\frac{\partial u}{\partial r}=0,\quad r=0;\qquad \frac{\partial u}{\partial r}+\alpha_1(z)[T(u)-T_w]=0,\quad r=a;\qquad (30)$$

$$\frac{\partial u}{\partial z}-\alpha_2(r)[T(u)-T_w]=0;\qquad \frac{\partial u}{\partial z}=q(r)-f(T(u)),\quad z=l.$$

Because Green's function of a linear boundary problem corresponding to problem (30) does not exist then representing the boundary condition on the surface $r=a$ in the form

$$\frac{\partial u}{\partial r}+hu=hu-\alpha_1(z)[T(u)-T_w],\quad r=a;\quad 0<z<l;\quad (0<h<\infty),$$

we can formulate the boundary problem for an auxiliary Green function $G_a(r,z;\rho,x)$

$$\frac{1}{r}\frac{\partial}{\partial r}\left(r\frac{\partial G_a}{\partial r}\right)+\frac{\partial^2 G_a}{\partial z^2}=-\delta(r-\rho)\delta(z-x),\quad 0<r,\rho<a,\ 0<z,x<l;$$

$$\frac{\partial G_a}{\partial r}=0,\quad r=0;\qquad \frac{\partial G_a}{\partial r}+hG_a=0,\quad r=a;\qquad \frac{\partial G_a}{\partial z}=0,\quad z=0,\ z=l,$$

the solution of which is of the form

$$G_a(r,z;\rho,x)=\frac{1}{a^2}\sum_{n=1}^{\infty}G_n(x,z)J_0(\gamma_n\rho)J_0(\gamma_n r)/P_n,$$

$$G_n(x,z)=\gamma_n\exp[-\gamma_n(z-x)][1+\exp(-2\gamma_n x)][1+\exp(-2\gamma_n(l-z))],\ x\le z;$$

$$G_n(z,x)=G_n(x,z);\qquad P_n=(\gamma_n^2+h^2)[1-\exp(-2\gamma_n l)]J_0^2(\gamma_n a);$$

where $0<\gamma_1<\gamma_2<\ldots$ are roots of the equation $hJ_0(\gamma a)-\gamma J_1(\gamma a)=0$.

Introducing the following notations: $u(r,0)=v_0(r)$, $u(r,l)=v_1(r)$, $u(a,z)=w(z)$, after an application of the second Green formula we can express the unknown function $u(r,z)$ in terms of it values on the surfaces $z=0$, $z=l$ and $r=a$

$$u(r,z)=\int_0^a G_a(r,z;\rho,l)[q(\rho)-f(T(v_1(\rho)))]\rho d\rho+a\int_0^l G_a(r,z;a,x)[hw(x)-$$

$$-\alpha_1(x)[T(w(x))-T_w]]dx-\int_0^a G_a(r,z;\rho,0)\alpha_2(\rho)[T(v_0(\rho))-T_w]\rho d\rho.\quad (31)$$

Writing integral relation (31) for $z=0$, $z=l$ and $r=a$ consecutively we obtain a system of three integral Hammerstein equations concerning the function $v_0(r)$, $v_1(r)$ and $w(z)$. After approximate solving of this system by means of a projective-net method we can find $u(r,z)$ from (31).

The numerical solution of the integral equations system obtained from (31) is found in the case of the computation of a steady-state temperature regime for the EBAM of niobium in an autocrucible of diameter 280 mm ($a=0.14$ m) where a level of metal in which is equal to $l=0.14$ m. We have assumed that $\alpha_2(r)=0$, $R=0$, $b=0.04$ m, $\lambda_E=562.716$ W/(m·K). We have considered a linear dependence of the thermal conductivity coefficient $\lambda_s(T)$ on the temperature on the basis of the niobium thermal conductivity data [13]:

$\lambda_s(T) = \lambda_0 + \beta(T-T_w)$, $\lambda_0=53.7$ W/(m·K), $\beta=0.01063$, $T_w=300$ K.

In Fig.10 the sections of the solid-liquid interfaces $r=R(z)$ obtained for $\alpha_1=400$ W/(m^2·K) (curves 1-3) and for the two values of the electron-beam heating power being absorbed by metal, $P=130$ kW (continuous lines) and $P=65$ kW (dashed) in the cases of various representations of the thermal conductivity coefficient in the solid phase domain: $\lambda_s=54.1$ W/(m·K) (the value from [10], curve 1), $\lambda_s=66.2$ W/(m·K) (a mean value in the temperature interval from 300 K to 2740 K, curve 2) as well a linear dependence $\lambda_s=\lambda_s(T)$ (curve 3) are presented. The curves 4 and 5 correspond to the case where $\lambda_s=\lambda_s(T)$ and a linear dependence of the heat exchange coefficient $\alpha_1(z)$ on the coordinate z, moreover $\alpha_1(0)=300$, $\alpha_1(l)=500$ W/(m^2·K) (curve 4), and also the curve 5 corresponds to the values $\alpha_1(0)=200$, $\alpha_1(l)=600$ W/(m^2·K).

Thus, in consequence of taking account of a dependence of the thermal conductivity upon the temperature that is possible thanks to using of the auxiliary Green function method for the concerned example a refinement of the results of the calculation of the melt volume makes up from 10.9% (comparison of the curves 2 and 3) to 36.6% (comparison of the curves 1 and 3). Besides, the application of the auxiliary Green function method permits to take into account a change of the heat exchange coefficients on the autocrucible surfaces being cooled, that, in turn, for the preceding example leads

to a refinement of the results of the calculation of the melt volume by 5.7% (comparison of the curves 3 and 4) and by 10.2% (comparison of the curves 3 and 5).

If we shall compare the obtained values of the liquid pool volume and the results obtained for the constant value λ_s=66.2 W/(mK) on surface $r=a$ and a step dependence $\lambda_s=\lambda_s(T)$ into the solid phase domain, Ω_s, then we shall see such assumptions lead to exceeding of the volume for α_1=400 W/(m^{2}K), P=130 kW by 15.3% and by 9.8% for P=65 kW. In addition, the maximum exceeding of the metal temperature in the solid phase domain for P=130 kW attains 100 K and 40 K at the center of the focal spot on the surface being heated.

To verify a correspondence of the mathematical model described by Stefan problem (19) to real thermal EBAM regimes we have conducted a comparison of the computation results and known experimental data from [10]. In the case of the niobium experimental melting in an autocrucible of diameter 280 mm with using of the MEMS for the electron beam maximum power P_0=190 kW the mass of the obtained melt oscillates from 8.4 kg to 8.7 kg that is between 976.7 cm^3 and 1011.6 cm^3. In Fig.7 the curves $W(R)$ corresponding to the value P=133 kW intersect this band of values for the scan radius values between 3 and 5 cm.

According to [10] in the case of the EBAM without the forced stirring the pool depth of zirconium in an autocrucible of diameter 250 mm makes up 24-28 mm. According to our calculations for zirconium (a=0.125 m; l=0.1 m; α_1=400 W/(m^2·K); α_2=50 W/(m^2·K); v_m=0.005 m/s; b=0.03 m; R=0.35 м, λ and C_{vL} from [10]) the pool depth oscillates from 20 to 27.2 mm if the absorbed power is changed from P=52.5 kW to P=105 kW.

In [10] one has obtained experimental results for the zirconium melting in an autocrucible of diameter 215 mm for the maximum power P_0=102 kW (P=0.7P_0=71.4 kW). The autocrucible bottom has not been cooled. The discharge of the zirconium melt for the melting with the MEMS was equal to 10.7 kg (1648.7 cm^3) and without the MEMS one was equal to 3.1 kg (477.8 cm^3). To compare the results we have realized the calculations for the follows values of

the parameters: 1) a=0.1075 m; l=0.1 m; b=0.03 m; P=71.4 kW; α_1= 400 W/(m^2·K); α_2= 50 W/(m^2·K); v_m= 0.3 m/s; 3 cm ≤R≤ 6 cm; 2) a= 0.1075 m; l= 0.05 m; b=0.03 m; P=71.4 kW; α_1=400 W/(m^2·K); α_2=50 W/(м^2·K); v_m=0.005 m/s; 3 cm ≤R≤ 5.25 cm. In the first case the liquid pool volume is changed from 919 cm^3 to 1633 cm^3 and in the second case one is changed between 206 cm^3 and 464 cm^3.

In [14] one has established that the melt overheating over the melting temperature did not exceed 100 K for the stirring velocity in a liquid pool v_m=1 m/s. This result is well consistent with the values of the maximum temperature on the pool surface obtained by means of our numerical calculations. For niobium (a=l=0.14 m; b=0.03 m; P=133 kW; R=0.065 m) the maximum overheating is equal to 101-102 degrees and for the scan radius R=0.05 m one achieves 186 K. For zirconium (a=0.1075 m; l=0.11 м; b=0.03 m; P=71.4 kW) the maximum overheating is changed from 134 K (R=0.045 m) to 95 K (R=0.055 m).

Thus, the results obtained by means of computations are experimentally verified completely satisfactorily therefore the developed mathematical models can be used for technological investigations of the EBAM.

REFERENCES

1. A.A.Berezovsky & V.D.Dovbnia, Mathematical models of thermal processes in an autocrucible during the electron-beam autocrucible melting, *Nonlinear Boundary Problems*, pp.41-57. Inst.of Mathem., Kyiv (1980). (In Russian).
2. T.A.Andreyeva, A.A.Berezovsky & V.D.Dovbnia, Mathematical models of liquid pool formation in an autocrucible during the electron-beam autocrucible melting, *Stefan Problems in Special Electrometallurgy and Sea Physics* (Preprint / Acad.Scien.Ukrain. SSR. Inst.of Mathem.,86.19), pp.3-21. Kyiv (1986). (In Russian).
3. Yu.A.Mitropolsky & A.A.Berezovsky, Stefan problems with limit steady state in special electrometallurgy, cryosurgery and sea physics, *Math.Physics and Nonlinear Mechanics*, № 7, pp.50-60. Kyiv (1987). (In Russian).
4. T.A.Andreyeva, A.A.Berezovsky & V.D.Dovbnia, Dynamics of liquid pool formation in an autocrucible during the electron-beam autocrucible melting, *Mathematical Problems of Energetic*, pp.106-122. Nauk.Dumka, Kyiv (1998). (In Russian).
5. Yu.A.Mitropolsky, A.A.Berezovsky & T.A.Plotnitsky, Free boundary problems for nonlinear evolution equation in problems of metallurgy, medicine, ecology, *Ukrainian Mathem.Journ.*,44, 67-76 (1992). (In Russian).
6. Mitropolsky Yu.A., Berezovsky A.A., Berezovsky S.A. *Free Boundary Problems for Nonlinear Evolution Equations in Metallurgy, Medicine and Ecology*.- Kyiv, 1994.- 54 p.- (Preprint/ Nat. Acad. Scien.Ukraine. Inst.of Math.; 94.20).
7. A.A.Berezovsky Yu.V.Zhernovyi & M.T.Saychuk, Numerical investigation of steady-state thermal regime during the electron-beam autocrucible melting in the case of circular scan of a beam, *Problems of Special Electrometallurgy*, № 4, 18-25 (1995). (In Russian).
8. A.A.Berezovsky Yu.V.Zhernovyi & M.T.Saychuk, Mathematical modelling of steady-state thermal regime in an autocrucible during the electron-beam autocrucible melting, *Heat Physics of High Temperatures*, **34**, 125-133 (1996). (In Russian).
9. L.A.Volkhonsky, *Vacuum Arc Furnaces*. Energoatomizdat, Moscow (1985). (In Russian).

10.S.V.Ladokhin & Yu.V.Korniushin, *Electron-beam Autocrucible Melting of Metals and Alloys*. Nauk.Dumka, Kyiv (1988). (In Russian).
11.A.A.Uglov, I.Yu.Smurov & A.M Lashin, Modelling of nonstationary movement of phase boundaries during action of energy fluxes on materials, *Heat Physics of High Temperatures*, 27, 87-93 (1989). (In Russian).
12.R.M.Cherniga & I.G.Odnorozhenko, Investigation of melting and evaporation processes of metals during action of impulse series of laser radiation, *Industrial Heat Engeneering*, 13, № 4, 51-59 (1991). (In Russian).
13.A.N.Zelikman, B.G.Korshunov, A.V.Yeliutin & A.M. Zakharov, *Niobium and Tantalum*. Metallurgy, Moscow (1990). (In Russian).
14.Yu.P.Anikin, M.I.Taranov, N.M.Kochegura, S.V.Ladokhin, V.L.Shevtsov, Ye.A.Markovsky & S.P.Smirnov, Influence of electron-beam autocrucible melting on structure and properties of heat stable alloy ChS 70, *Problems of Special Electrometallurgy*, № 3, 40-43 (1993). (In Russian).

Contents

Научное издание

MITROPOLSKY YURI ALEKSEEVICH
BEREZOVSKY ARNOLD ANATOLIEVICH
ZHERNOVYI YURI VASYLIOVYCH

FREE BOUNDARY PROBLEMS AND MATHEMATICAL MODELLING OF ELECTRON-BEAM AUTOCRUCIBLE MELTING

МИТРОПОЛЬСКИЙ ЮРИЙ АЛЕКСЕЕВИЧ
БЕРЕЗОВСКИЙ АРНОЛЬД АНАТОЛЬЕВИЧ
ЖЕРНОВЫЙ ЮРИЙ ВАСИЛЬЕВИЧ

ЗАДАЧИ СО СВОБОДНОЙ ГРАНИЦЕЙ И МАТЕМАТИЧЕСКОЕ МОДЕЛИРОВАНИЕ ЭЛЕКТРОННО-ЛУЧЕВОЙ ГАРНИСАЖНОЙ ПЛАВКИ

Редактор Н.И.Коваленко

Подп. в печ. 29.10.97.Формат 60×84/16. Бумага тип. Офс.печать
Усл.печ.л. 2,09. Усл.кр.-отт. 3,09. Уч.изд.л. 1,6. Тираж 100 экз.
Зак.166.

Подготовлено и отпечатано в Институте математики НАН Украины

252601 Киев 4, ГСП, ул. Терещенковская, 3